Role of Magnetism in Catalysis

Torun, E.; Fang, C. M.; de Wijs, G. A.; de Groot, R. A.

Published in:
Journal of Physical Chemistry C

DOI:
10.1021/jp4020367

THE JOURNAL OF PHYSICAL CHEMISTRY C

Article

pubs.acs.org/JPCC

Role of Magnetism in Catalysis: RuO_2 (110) Surface

E. Torun,[†] C. M. Fang,[†] G. A. de Wijs,[†] and R. A. de Groot*[,†,‡]

[†]Electronic Structure of Materials, Institute for Molecules and Materials, Radboud University Nijmegen, Heyendaalseweg 135, 6525 AJ, Nijmegen, The Netherlands

[‡]Laboratory of Chemical Physics, Zernike Institute of Advanced Materials, Nijenborgh 4, NL-9747 AG Groningen, The Netherlands

ABSTRACT: Angular momentum seems to not be conserved in chemical reactions where *one* of the reactants is magnetic; consequently, such reactions show a high activation barrier. An example is the production of hydrogen by electrolysis of water: practically all losses occur in the production of (magnetic) oxygen. Anodes with a low overvoltage (a measure of the losses) are based on the ruthenium dioxide (110) surface. First-principles electronic structure calculations show that this surface itself carries magnetic moments. This magnetic surface enables the production of oxygen in the ground state while conserving angular momentum.

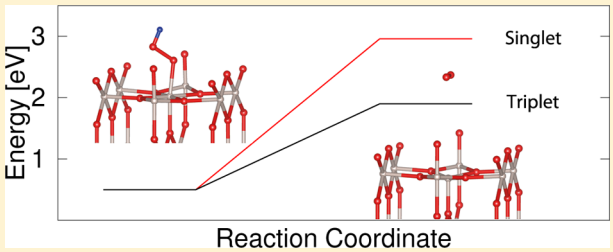

INTRODUCTION

Electrolysis of water is a potential source of hydrogen on a large scale. A measure of the inefficiency in electrolysis is the overvoltage, the voltage needed to drive the process in excess of the voltage under thermodynamical equilibrium conditions. The contribution to the overvoltage of the oxygen evolution dominates overwhelmingly. One of the best anodes in this respect is based on the RuO_2 (110) surface, and improvements have been reported, such as, by the partial substitution of ruthenium by tungsten,[1] cobalt,[2] and nickel.[3]

Because oxygen evolution produces magnetic oxygen from nonmagnetic water, the inclusion of the effects of surface magnetism could be highly relevant.[4] Because neither water nor hydrogen is magnetic, on a nonmagnetic anode the oxygen can be produced only in an excited nonmagnetic state without violating conservation of angular momentum. The two lowest excited states of the oxygen molecule are singlet states, $^1\Delta_g$ and $^1\Sigma_g$, 1 and 1.6 eV above the $^3\Sigma_g$ ground state.[5] For nonmagnetic anodes, we associate the high overvoltage with the notion that oxygen is produced initially in its nonmagnetic excited state and decays slowly to the ground state by higher order processes. A detailed study of the energetics of the oxygen evolution on the RuO_2 (110) surface was reported by Rossmeisl et al.[6] This work did not include the influence of magnetism, however.

Here we report on the local electronic and magnetic properties of RuO_2 (110) surfaces. We show that the RuO_2 (110) surface is magnetic. This is an unexpected property because the bulk RuO_2 is not magnetic. Magnetism in 4d and 5d metals and their compounds is rare but not unique;[7−9] for example, magnetic properties of RuO_2 nanoparticles have been investigated.[10,11] The surface magnetism that we report here is an important property because it provides us the necessary degree of freedom to allow the production of oxygen in its magnetic ground state while conserving angular momentum.

DETAILS OF THE CALCULATIONS

Experimental[12−15] and theoretical analyses[16−24] show that the RuO_2 (110) surface has two different ruthenium atoms, one with six-fold coordination by oxygen (Ru6) and one with a five-fold coordination (Ru5). The latter is regarded as the active site in catalysis.[12−24] Previous studies have focused on surface morphologies and local atomic structure. Scheffler et al. found that the clean surface exists in an oxygen-poor environment, whereas in an environment rich in oxygen the stable form of the RuO_2 (110) surface has terminal oxygen on top of the Ru5 atoms.[19−22]

RuO_2 can be regarded as consisting of alternate layers of oxygen and Ru_2O_2 layers along the (110) direction. We cleave the crystal in the O atomic layer; a surface oxygen atom bridges two Ru6 atoms. There are two distinct ruthenium atoms in the (110) surface: a six-fold-coordinated (Ru6) and a five-fold-coordinated (Ru5), as shown in Figure 1a. A unit cell of 3.14 Å × 6.43 Å × 25.00 Å containing 24 atoms in 9 atomic layers in a slab and 12 Å vacuum between them was employed.

Calculations were carried out using the first-principles code Vienna ab initio simulation program (VASP)[25−28] employing density functional theory (DFT), and the projector-augmented wave (PAW) method.[29,30] The generalized gradient approximation (GGA) by Perdew, Burke, and Ernzerhof (PBE)[31,32] was employed for the exchange and correlation potentials. The quantization axis for the spin is taken along the z direction. The Brillouin-zone integration used 8 × 8 × 12 *k*-mesh or 105 *k*-points in the irreducible Brillouin zone (BZ) of bulk RuO_2. For the (110) surface systems the electronic wave functions were sampled on 12 × 6 × 1 *k*-mesh or 28 *k*-points in the irreducible BZ. The cutoff energy of the wave functions was 500 eV. The cutoff energy of the augmentation funtions was 605 eV, and for the smearing we used Gaussian method. The structure was

Received: February 27, 2013
Published: March 7, 2013

   dx.doi.org/10.1021/jp4020367 | *J. Phys. Chem. C* 2013, 117, 6353−6357

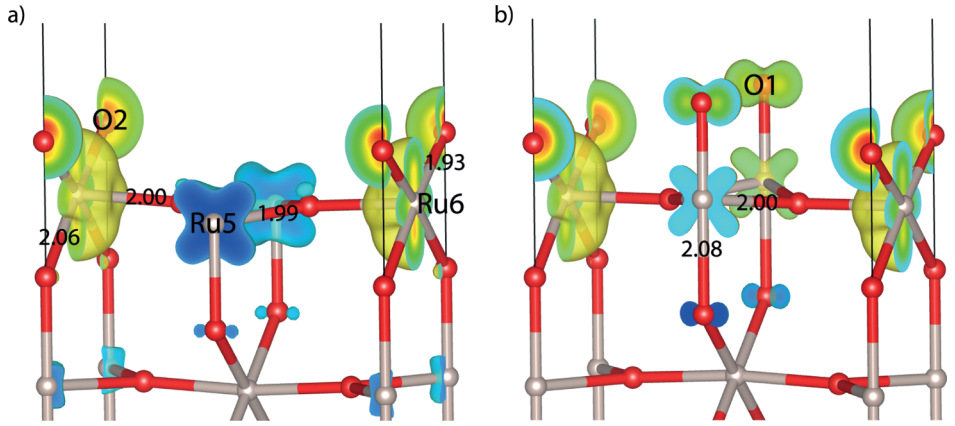

Figure 1. Local coordination and the spin density of the RuO_2 (110) surfaces. Blue corresponds to negative; red corresponds to positive spin density. (a) Bridging O (O2) atoms, six-fold-coordinated Ru atoms (Ru6), and five-fold-coordinated Ru atoms (Ru5). (b) Surface with oxygen coverage: the Ru5 covered by one O (O1). The numbers represent the Ru−O bond lengths (in angstroms).

optimized until all forces were smaller than 0.01 eV/Å . The convergences of the cutoff energies and *k*-meshes have been verified.

CLEAN RuO_2 (110) SURFACE

The results of structural relaxations of bulk RuO_2 are in line with former calculations;[33,34] see Table 1. Calculations for the relaxed RuO_2 (110) surface using the spin-polarizated DFT-GGA method resulted in a magnetic solution 38 meV lower in total energy compared with the nonmagnetic solution. The spin-polarization is confined to the surface atoms: 0.60 μ_B for Ru6, −0.24 μ_B for Ru5, and 0.19 μ_B at the bridging oxygen site (O2). (See Table 2.) The total magnetization of each surface of the slab is 0.55 μ_B. Figure 2 reveals the origin of the surface magnetism: it shows the partial density of the surface ruthenium 4d and oxygen 2p states around the Fermi level for the nonmagnetic and the magnetic cases. Both nonmagnetic densities of states peak at the Fermi level. The density of states at the Fermi level for Ru6 is 1.1 states/eV compared with 0.7 states/eV in the bulk. Hence this surface fullfills the Stoner criterion for magnetism, unlike the bulk. The spin-polarization causes a moderate splitting of the density of states of the Ru5 4d states, consistent with its magnetic moment (about −0.24 μ_B). The widths (8.2 eV) of the subsurface ruthenium 4d and oxygen 2p states are close to those of the bulk. However, the shape of the partial density of the surface ruthenium 4d states is significantly different from that of the bulk due to a different crystal field splitting.

The O2 2p states have a density of ∼0.80 states/eV per atoms at the Fermi level. That is significantly larger than those in the subsurface layer and bulk (typically around 0.2 states/eV per atom). Calculations show a spin splitting of about 0.8 eV with a peak at about −0.3 eV for the spin-up electrons and another peak at about 0.5 eV for the spin-down electrons. As a result, there is a magnetic moment of ∼0.19 μ_B at the bridging oxygen site. The spin-polarization shows little effect on the subsurface O atoms.

Table 1. Calculated Results (Lattice Parameters and Coordinates of Oxygen Atoms) of Bulk RuO_2 Rutile Using the DFT-GGA Method

	this work	previous calculations	experiments
a (Å)	4.55	4.554,[33] 4.56[34]	4.51,[35] 4.4919,[36] 4.4906[37]
c (Å)	3.14	3.137, 3.16	3.11, 3.1066, 3.1064
c/*a*	0.69	0.6888, 0.6930	0.6896, 0.6916, 0.6918
u(O)	0.306	0.3054, 0.3067	0.3058
V_0(Å/fu)	32.42	32.53, 32.10	31.63, 31.32, 31.32

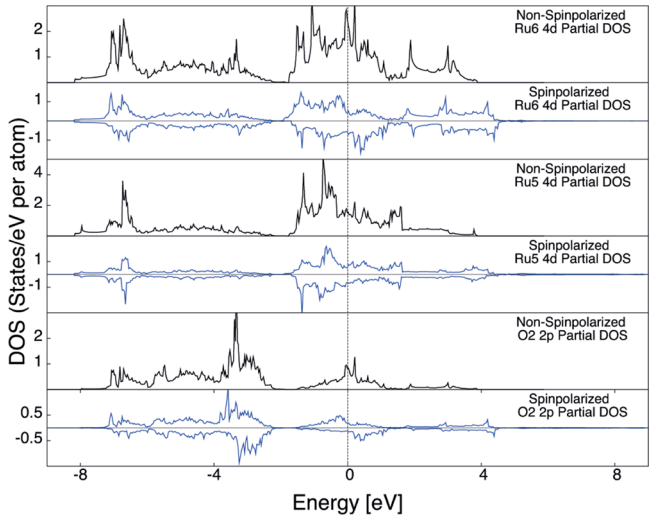

Figure 2. Partial density of states of the surface O and Ru states on RuO_2 (110) showing the effect of spin polarization. Remark the maxima at the Fermi energy for several nonspinpolarized cases.

Table 2. Surface Energy and Local Moments of RuO_2 Rutile (110) and (110)-O Surfaces Using the DFT-GGA Method

	moment (μ_B)				E_{surf} (J/m^2)		
	Ru5	Ru6	O2	O1	present	literature	E_{sp}-E_{nm} (meV/cell)
(110)	−0.24	0.60	0.19		1.04	1.14,[15] 1.03[16]	−38
(110)-O	0.10	0.69	0.29	0.14			−53

dx.doi.org/10.1021/jp4020367 | J. Phys. Chem. C 2013, 117, 6353−6357

Because surface magnetism is a subtle effect, we also performed WIEN2k[38] calculation for clean RuO_2 (110) surface to make a benchmark. We chose Wien2k for benchmarking because WIEN2k and VASP are different DFT methods. WIEN2k is a full potential linearized augmented plane wave (LAPW) method where VASP is a plane-wave pseudopotential metod. For WIEN2k calculations, a 3.14 Å × 6.43 Å × 25.00 Å unit cell was used that contains 24 atoms in 9 atomic layers and also more than 12 Å vacuum. This is the same unitcell that we used in VASP calculations. The electronic wave functions were sampled on 12 × 6 × 1 *k*-mesh or 18 *k*-points in the irreducible BZ using the Monkhorst-Pack method.[39] To make a reasonable comparison between these two different methods, we optimized the cell with WIEN2k and used the optimized geometry as a starting guess for VASP. For relaxation in VASP, we used the same parameters, for example, convergence criteria, *k*-point generation scheme, and atomic radii for local magnetic moments, as we used in WIEN2k. Finally, we observed that the relaxed geometries for VASP and WIEN2k are almost the same and total magnetic moments per surface unit cell for VASP and WIEN2k are close to each other, 0.56 and 0.52, respectively, which we consider to be a good agreement. So, WIEN2k calculations confirmed that the RuO_2 (110) surface is magnetic.

O-COVERED RuO_2 (110) SURFACE

The addition of oxygen on top of Ru5 (Figure 1b) has a profound influence; see Table 2. The Ru5 shifts 0.09 Å outward, in contrast with the clean surface, where it moved 0.07 Å inward. The new Ru−O bond is short, 1.73 Å, on the expense of the Ru−O bond to the oxygen below, which expands from 1.90 Å in the clean surface to 2.08 Å in the case of an extra oxygen. The addition of an oxygen atom on top of the Ru5 atom slightly perturbs the local coordination of the Ru6 atom. The Ru6 atom and the bridging O atom move slightly inward. The magnetic ground state is more stable by 53 meV compared with the nonmagnetic case, which is 15 meV more compared with the case without oxygen coverage.

Figure 3 shows the calculated partial density of the ruthenium 4d and oxygen 2p states at the oxygen-covered surface. The peak positions and widths of the densities of states of the Ru6 4d and the bridging O 2p states are basically the same as those of the clean surface. For the nonmagnetic case, the density of states peaks at the Fermi level for both the ruthenium 4d as well as the oxygen 2p states (as it does for the clean surface). Spin-polarization has a significant influence on these partial densities of states.

The partial density of the Ru5 4d states of the oxygen-covered surface has a significant different shape as compared with that of the clean surface (Figures 2 and 3). There are two strong peaks at about −1.0 and +0.4 eV. The latter peak corresponds to the peak from the 2p states of the terminal oxygen atom. Spin-polarization has much less influence on the Ru5 4d and terminal O (O1) 2p states. The magnetic moments of the Ru6 and Ru5 are parallel, in contrast with the case of the clean surface.

On the oxygen-covered RuO_2 (110) surface, the local magnetic moments of the Ru6 and bridging O atoms are close to those for the clean surface. The moment of the Ru5 on the oxygen-covered surface remains very small (~0.1 μ_B) but aligns parallel. Therefore, the total magnetic moment of the oxygen-covered surface increases to 1.22 μ_B per unit cell on one oxygen-covered surface and from 0.55 μ_B per unit cell on a clean (110) surface.

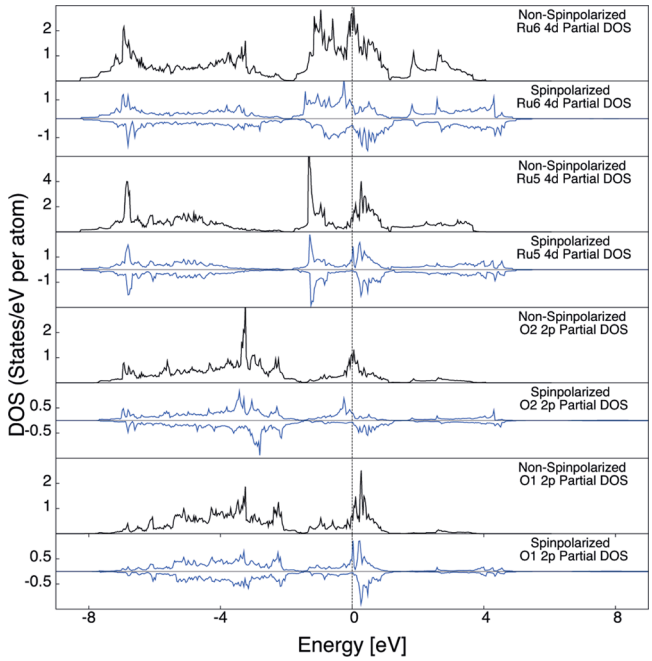

Figure 3. Partial density of states of the surface O and Ru states on RuO_2 (110) with oxygen coverage on top of Ru5, showing the effect of spin polarization.

ROLE OF SURFACE MAGNETISM IN ELECTROLYSIS OF WATER

The reaction path of water electrolysis on ther 2 × 1 RuO_2 (110) surface was suggested by Rossmeisl et al.[6] Because O_2 is produced as a final product of water electrolysis, the conservation of angular momentum and the surface magnetism are playing a vital role mostly at the final step of this reaction path. That is why to elucidate the importance of the surface magnetism for electrolysis of water we performed DFT total energy calculations for the last step of this reaction path. In Figure 4, the initial and the final states of the final step of electrolysis of water can be seen. Initially, OOH was adsorbed on the coordinately unsaturated point of the 2 × 1 RuO_2 (110) surface; finally, O_2 desorbs from the surface after the removal of the H atom.

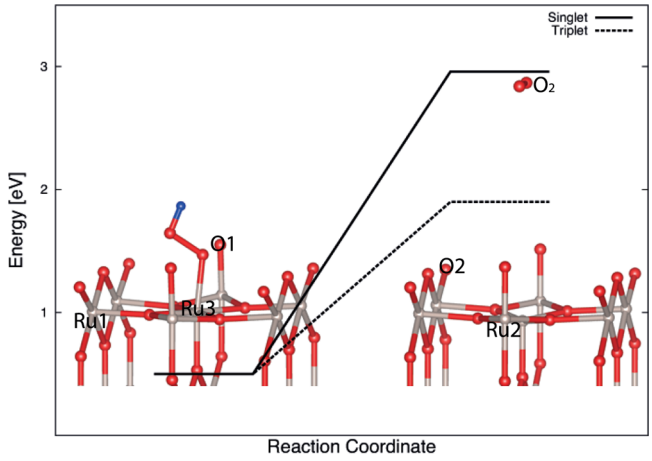

Figure 4. Calculated total energy change for the last step of the water electrolysis, for magnetic ("Triplet") and nonmagnetic ("Singlet") anode. The energy of $1/2H_2$ is added to the final-state total energies.

dx.doi.org/10.1021/jp4020367 | J. Phys. Chem. C 2013, 117, 6353−6357

We performed two different sets of calculations that we named "Singlet" and "Triplet". In the "Singlet" case, we assumed that the RuO_2 (110) surface is not magnetic so the O_2 molecule should be produced initially in its nonmagnetic singlet excited state. For this scenario, we obtained the total energy difference between these two states from nonspinpolarized DFT calculations and labeled it as "Singlet" in Figure 4. For the "Triplet" case, surface magnetism enables the production of oxygen in its magnetic ground state. First, we performed spin-polarized DFT calculation to find the local and total magnetic moments of the initial state (Table 3). Then, we fixed the total spin angular momentum of the unitcell and tried to obtained O_2 molecule in its triplet magnetic ground state for the final step. We observed that surface atoms rearrange their moments to conserve total spin angular momentum in the unitcell while obtaining O_2 molecule in its magnetic ground state. We also observed that the total energy change in the "Triplet" case is ∼1 eV *lower* in energy than the "Singlet" case, which can be seen in Figure 4.

Table 3. Total and Local Magnetic Moments for the Initial and the Final States of the Last Step of the Water Electrolysis

	moment (μ_B)						
	Ru1	Ru2	Ru3	O1	O2	O_2	total
initial	0.49	0	0	0	0.17		2.41
final	−0.49	−0.22	0	−0.24	−0.19	2	2.41

CONCLUSIONS

Magnetism usually occurs in materials containing elements where a certain angular momentum appears first. The orthogonality of the valence electrons (that carry the magnetic moment) to the core is always fulfilled, so no constraints exist on the radial Schrödinger equation (any constraint increases the energy and hence the delocalization of these states), but several exceptions exist; for example, strontiumruthenate is ferromagnetic. In general, surfaces with atoms with a lower coordination show an increased tendency toward magnetism. Magnetism is the rule rather than the exception in isolated atoms, but also isolated 4d atoms in an alkali−metal matrix show local moments.[40]

The calculations presented here show that both the (110) stoichiometric and the oxygen-covered surfaces of ruthenium-dioxide show local magnetic moments. The relevance of the surface magnetism reported in this article is in electrolysis, so how surface magnetism can be important for electrolysis of water is also illustrated.

The spin-conservation rule (which we call angular momentum conservation) is a key selection rule for chemical reactions.[41] The importance of the spin-selection rule can be seen in Scheffler's work.[42] They concluded the origin of the low sticking parameter of O_2 on Al(111) is having O_2 in a triplet and the Al(111) surface in a singlet state. Another example is a recent review where Metiu pointed out that from a quantum mechanics point of view reactions in which the total spin of the reactants differs from the total spin of the products are very slow.[4]

A comparison with the most fundamental form of oxygen-evolution, photosynthesis, is in order here. In photosynthesis, carbon dioxide and water are transformed into oxygen and organic compounds by sunlight, a process in which magnetic oxygen is the only magnetic reactant as well. Photosynthesis is *impossible* without traces of manganese. The production of oxygen in photosynthesis is a four-step process that involves a polynuclear, magnetic cluster containing four manganese ions.[43] A second magnetic entity seems ubiquitous in the production of molecular oxygen.

AUTHOR INFORMATION

Corresponding Author

*E-mail: r.degroot@science.ru.nl.

Notes

The authors declare no competing financial interest.

ACKNOWLEDGMENTS

Dr. Remco Havenith is acknowledged for the discussions. This work is a part of the research programs of NanoNed and the Stiching voor Fundamenteel Onderzoek der Materie (FOM) with financial support from the Nederlandse Organisatie voor Wetenschappelijk Onderzoek (NWO).

REFERENCES

(1) Shafer, M. W.; De Groot, R. A. *IBM Tech. Discl. Bull.* **1979**, *21*, 5070.
(2) Jirkovsky, J.; Makarova, M.; Krtil, P. *Electrochem. Commun.* **2006**, *8*, 1417−1422.
(3) Macounova, K.; Jirkovsky, J.; Makarova, M. V.; Franc, J.; Krtil, P. *J. Solid State Electrochem.* **2002**, *13*, 959−965.
(4) Chretien, S.; Metiu, H. *J. Chem. Phys.* **2008**, *129*, 074705.
(5) Bytautas, L.; Matsunaga, N.; Ruedenberg, K. *J. Chem. Phys.* **2010**, *132*, 074307.
(6) Rossmeisl, J.; Qu, Z. W.; Zhu, H.; Kroes, G. J.; Norskov, J. K. *J. Electroanal. Chem.* **2007**, *607*, 83−89.
(7) Longo, J.; Raccah, P. M.; Goodenough, J. B. *J. Appl. Phys.* **1968**, *39*, 1327−1328.
(8) Eriksson, O.; Albers, R. C.; Boring, A. M. *Phys. Rev. Lett.* **1991**, *66*, 1350−1353.
(9) De Boer, P. K.; De Groot, R. A. *Phys. Rev. B* **1999**, *59*, 9894−9897.
(10) Diaz, C.; Valenzuela, M. L.; Spodine, E.; Moreno, Y.; Pena, O. *J. Cluster Sci.* **2007**, *18*, 831−844.
(11) Biswas, K.; Rao, C. N. R. *J. Nanosci. Nanotechnol.* **2007**, *7*, 1969−1974.
(12) Over, H.; Seitsonen, A. P.; Lundgren, E.; Schmid, M.; Varga, P. *Surf. Sci.* **2002**, *515*, 143−156.
(13) Over, H. *Appl. Phys. A* **2002**, *75*, 37−44.
(14) Over, H.; Muhler, M. *Prog. Surf. Sci.* **2003**, *72*, 3−17.
(15) Kim, Y. D.; Schwegmann, S.; Seitsonen, A. P.; Over, H. *J. Phys. Chem. B* **2001**, *105*, 2205−2211.
(16) Wang, H.; Schneider, W. F. *J. Chem. Phys.* **2007**, *127*, 064706.
(17) Liu, P.; Muckerman, J. T.; Adzic, R. R. *J. Chem. Phys.* **2006**, *124*, 141101.
(18) Kiejna, A.; Kresse, G.; Rogal, J.; De Sarkar, A.; Reuter, K.; Scheffler, M. *Phys. Rev. B* **2006**, *73*, 035404.
(19) Reuter, K.; Scheffler, M. *Phys. Rev. B* **2002**, *65*, 11.
(20) Reuter, K.; Ganduglia-Pirovano, M. V.; Stampfl, C.; Scheffler, M. *Phys. Rev. B* **2002**, *65*, 165403.
(21) Reuter, K.; Scheffler, M. *Phys. Rev. B* **2003**, *68*, 045407.
(22) Reuter, K.; Scheffler, M. *Phys. Rev. Lett.* **2003**, *90*, 046103.
(23) Sun, Q.; Reuter, K.; Scheffler, M. *Phys. Rev. B* **2003**, *67*, 205424.
(24) Temel, B.; Meskine, H.; Reuter, K.; Scheffler, M.; Metiu, H. *J. Chem. Phys.* **2007**, *126*, 204711.
(25) Kresse, G.; Hafner, J. *Phys. Rev. B* **1993**, *47*, 222−229.
(26) Kresse, G.; Hafner, J. *Phys. Rev. B* **1994**, *49*, 14251−14269.
(27) Kresse, G.; Furthmuller, J. *Comput. Mater. Sci.* **1996**, *6*, 15−50.
(28) Kresse, G.; Furthmuller, J. *Phys. Rev. B* **1996**, *54*, 11169−11186.
(29) Kresse, G.; Joubert, D. *Phys. Rev. B* **1999**, *59*, 1758−1775.
(30) Blöchl, P. E. *Phys. Rev. B* **1994**, *50*, 17953−17979.

(31) Perdew, J. P.; Burke, K.; Ernzerhof, M. *Phys. Rev. Lett.* **1996**, *77*, 3865−3868.
(32) Perdew, J. P.; Burke, K.; Ernzerhof, M. *Phys. Rev. Lett.* **1997**, *78*, 1396−1396.
(33) Tse, J. S.; Klug, D. D.; Uehara, K.; Li, Z. Q.; Haines, J.; Leger, J. M. *Phys. Rev. B* **2000**, *61*, 10029−10034.
(34) Glassford, K. M.; Chelikowsky, J. R. *Phys. Rev. B* **1993**, *47*, 1732−1741.
(35) Wyckoff, R. W. G. *Crystal Structures*; Interscience Publishers: New York, 1963; Vol. *1*.
(36) Boman, C. E. *Acta Chem. Scand.* **1970**, *24*, 116−122.
(37) Rogers, D. B.; Shannon, R. D.; Sleight, A. W.; Gillson, J. L. *Inorg. Chem.* **1969**, *8*, 841−849.
(38) Blaha, P.; Schwarz, K.; Madsen, G.; Kvasnicka, D.; Luitz, J. *WIEN2k: An Augmented PlaneWave + Local Orbitals Program*; Institut für Physikalische und Theoretische Chemie: Wien, Austria, 2001.
(39) Monkhorst, H. J.; Pack, J. D. *Phys. Rev. B* **1976**, *13*, 5188−5192.
(40) Riegel, D.; Gross, K. D.; Luszikbhadra, M. *Phys. Rev. Lett.* **1987**, *59*, 1244−1247.
(41) Wigner, E. *Nachr. Ges. Wiss. Goettingen, Math.-Phys.* **1927**, 375−381.
(42) Behler, J.; Delley, B.; Lorenz, S.; Reuter, K.; Scheffler, M. *Phys. Rev. Lett.* **2005**, *94*, 036104.
(43) Yachandra, V. K.; Sauer, K.; Klein, M. P. *Chem. Rev.* **1996**, *96*, 2927−2950.